

# Effects of temperature-dependent viscosity on Bénard convection in a porous medium using a non-Darcy model

K. Hooman<sup>\*</sup>, H. Gurgenci

*School of Engineering, The University of Queensland, Brisbane, Australia*

Received 19 December 2006; received in revised form 24 April 2007

Available online 27 September 2007

## Abstract

Temperature-dependent viscosity variation effect on Bénard convection, of a gas or a liquid, in an enclosure filled with a porous medium is studied numerically, based on the general model of momentum transfer in a porous medium. The exponential form of viscosity–temperature relation is applied to examine three cases of viscosity–temperature relation: constant ( $\mu = \mu_C$ ), decreasing (down to  $0.13\mu_C$ ) and increasing (up to  $7.39\mu_C$ ). Effects of fluid viscosity variation on isotherms, streamlines, and the Nusselt number are studied. Application of the effective and average Rayleigh number is examined. Defining a reference temperature, which does not change with the Rayleigh number but increases with the Darcy number, is found to be a viable option to account for temperature-dependent viscosity variation.

© 2007 Published by Elsevier Ltd.

*Keywords:* Temperature-dependent viscosity; Natural convection; Porous medium; Nusselt number; Bénard problem

## 1. Introduction

With interesting industrial applications such as filters and catalytic reactors, underground contaminant transport, oil and gas exploration and extraction, and grain storage, natural convection in porous media is a topic of increasing importance. The buoyancy-induced flow in a cavity heated from below leads to patterns of convection cells. The direction of fluid rotation alternates between neighboring cells. Known in the literature as the Bénard convection, the fluid motion starts only when the imposed temperature difference exceeds a certain value. The imposed temperature difference is generally represented by the dimensionless Rayleigh number. The critical Rayleigh–Darcy number, which indicates the onset of Bénard convection, is known to be equal to  $4\pi^2$  for the Darcy flow in a porous medium bounded by two infinite horizontal isothermal plates. This problem is sometimes referred to

as the Darcy–Bénard problem. Fundamentally, the momentum transport process in a porous medium is subject to additional viscous and quadratic inertial effects, representing deviations from the familiar Darcy law. The effects of the quadratic inertia and the viscous terms on natural convection were investigated by Lauriat and Prasad [1], Kladias and Prasad [2], Khashan et al. [3], and Lage [4]. On the other hand, the pioneering work of Vafai and Tien [5], which was later revisited by Hsu and Cheng [6], is widely accepted for using the volume-averaging technique coupled with semi-empirical formulas to arrive at the two-dimensional momentum equation. Later reports of Merrikh and co-workers [7–9] have elaborated on the application of the above method, to name a few.

Modeling heat transfer in a porous medium, in its turn, is a challenging problem. Involving various presumptions and simplifications, formulating the thermal energy equation is a continuous source of dispute and discussion as reflected in the large number of papers on the topic [10–23].

Our review of literature has indicated that most of the reported studies on Bénard convection assume constant viscosity. However, the fluid viscosity usually has a strong

<sup>\*</sup> Corresponding author. Tel.: +61 73365 3668; fax: +61 73365 4799.  
E-mail address: [k.hooman@ug.edu.au](mailto:k.hooman@ug.edu.au) (K. Hooman).

## Nomenclature

$b$	viscosity variation number	$x^*$	horizontal coordinate, m
$C_F$	inertia coefficient	$x$	$x^*/L$
$Da$	the Darcy number, $Da = K/L^2$	$y^*$	vertical coordinate, m
$E$	error in calculating $Nu$ based on effective/average $Ra$ , $ Nu - Nu_{\text{eff/am}} /Nu$	$y$	$y^*/L$
$e_{Nu}$	error in calculating $Nu$ based on reference temperature approach $e_{Nu} =  Nu - Nu^* /Nu$	<i>Greek symbols</i>	
$e_{\psi_{\text{max}}}$	error in calculating $\psi_{\text{max}}$ based on reference temperature approach $e_{\psi_{\text{max}}} =  \psi_{\text{max}} - \psi_{\text{max}}^* /\psi_{\text{max}}$	$\alpha$	thermal diffusivity of the porous medium, $\text{m}^2/\text{s}$
$g$	gravitational acceleration, $\text{m/s}^2$	$\beta$	thermal expansion coefficient, $\text{K}^{-1}$
$k$	porous medium thermal conductivity, $\text{W/m K}$	$\Gamma_\varphi$	diffusion parameter, $\text{m}^2/\text{s}$
$K$	permeability, $\text{m}^2$	$\Lambda$	inertial parameter $\Lambda = C_F L \phi^2 / (Pr_C \sqrt{K})$
$L$	cavity height, m	$\theta$	dimensionless temperature $(T^* - T_C)/(T_H - T_C)$
$Nu$	the Nusselt number	$\eta$	kinematic viscosity ratio
$Nu^*$	the Nusselt number with viscosity at reference temperature	$\mu$	fluid viscosity, $\text{N s/m}^2$
$P^*$	pressure, Pa	$\rho$	fluid density, $\text{kg/m}^3$
$Pr_C$	modified Prandtl number, $Pr_C = \phi v_C / \alpha$	$\nu$	kinematic viscosity, $\text{m}^2/\text{s}$
$Ra$	Rayleigh–Darcy number, $Ra = Da Ra_f$	$\varphi$	generic variable
$Ra_f$	the fluid Rayleigh number, $Ra_f = g\beta(T_H - T_C)L^3/(v_C\alpha)$	$\psi$	stream-function
$S_\varphi$	source term for $\varphi$ equation	$\psi_{\text{max}}$	maximum value of stream-function
$S_W$	source term for vorticity transport equation	$\psi_{\text{max}}^*$	$\psi_{\text{max}}$ with viscosity at reference temperature
$T^*$	temperature, K	$\phi$	porosity
$u^*$	$x^*$ -velocity, $\text{m/s}$	$\omega$	vorticity
$u$	$u^*L/\alpha$	<i>Subscripts</i>	
$ U^* $	mean velocity $\sqrt{u^{*2} + v^{*2}}$ , $\text{m/s}$	am	arithmetic mean
$ U $	dimensionless mean velocity $\sqrt{u^2 + v^2}$	ave	average
$v^*$	$y^*$ -velocity, $\text{m/s}$	C	of cold wall
$v$	$v^*L/\alpha$	cp	constant property
		eff	effective
		H	of hot wall
		ref	of reference temperature

dependence on temperature. For example, the viscosity of glycerin has a threefold decrease in magnitude for a 10 °C rise in temperature. This trend is not only observed in highly viscous liquids, such as glycerin, but can also happen in other fluids such as water where the viscosity decreases by about 240% when the temperature increases from 10 °C to 50 °C. Such severe changes in the fluid viscosity will result in different heat and fluid flow patterns compared to constant property solutions [24]. Some authors (see for example [25–28]) have investigated natural convection with temperature-dependent viscosity while keeping the other fluid properties constant (this assumption is known to be valid for some fluids [29]).

A relatively important problem is the study of ore body formation and mineralization in hydrothermal systems for which the temperature-dependent viscosity variation should be considered as noted by Lin et al. [24] who reported analytical solutions, backed by some numerical simulations, to claim that the viscosity variation effects will destabilize the Darcy–Bénard convection. The reference viscosity adopted in their Rayleigh–Darcy number was based on the cold wall conditions.

On the other hand, in a notable study, commenting on [25–27], Nield [30,31] argued that the effect of property variation on free convection is artificial and should disappear if one uses an effective Rayleigh number based on mean values. Nield [31] showed that, if the mean values are used, the critical Rayleigh number remains unaltered, which indicates that the flow of a fluid with temperature-dependent viscosity is no less stable than a constant property one. The convection does not start at a smaller Rayleigh number with a variable property fluid as long as proper care is applied when calculating the Rayleigh number. He also concluded that when the viscosity varied within one order of magnitude, the concept of effective Rayleigh number would work while it was conceded that possible localized flow in a part of the flow region might invalidate this argument if the property variation were more severe. It is interesting to note that, in an example of a fluid clear of solid material, for natural convection of corn syrup with a temperature-dependent viscosity, even extreme viscosity variations, did not have a significant effect on the overall heat transfer coefficient provided the properties were evaluated at the mean temperature and a correction factor was used

[32]. This conclusion is in line with what was reported for natural convection of air in a square enclosure [33]. Siebers et al. [34] have come up with the same conclusion for laminar natural convection of air along a vertical plate. Interestingly, they had to apply a correction factor on their Nusselt number for more intense convection case with the flow becoming turbulent.

The problem becomes more complicated when one observes that Guo and Zhao [28] evaluated the fluid properties at the arithmetic mean temperature (the mean of hot and cold wall temperatures in a laterally heated box) but their results still showed significant differences between constant- and variable property flows. For example, for  $Da = 10^{-4}$  and  $Ra = 10$ , the Nusselt number was about 75% higher than the constant property case.

This gives us the impression that more work on the issue is called for. A numerical simulation of the problem is presented here to investigate the effects of temperature-dependent viscosity on natural convection in a square porous cavity. The well-known problem of Bénard convection in a porous cavity is undertaken based on a non-Darcy flow model similar to that of [9]. However, our work is different from the previous studies addressing the variable viscosity effects on the Bénard convection as we considered the general model including the viscous and (both quadratic and convective) inertia terms. Several models have been used in the literature to account for the viscosity variation with the temperature. The exponential form of viscosity–temperature behavior is reported to be quite effective for most common fluids [35]. This model is applied here for flow of an incompressible gas or liquid. The viscosity of a gas usually increases with temperature and the viscosity of a liquid does the reverse. Both cases are considered here.

## 2. Model equations

Incompressible natural convection of a fluid with temperature-dependent viscosity in a square enclosure filled with homogeneous, saturated, isotropic porous medium with the Oberbeck–Boussinesq approximation for the density variation in the buoyancy term is considered, as shown in Fig. 1. It is assumed that the solid matrix and the fluid are in local thermal equilibrium. The equations that govern the conservation of mass, momentum and energy can be written as follows

$$\frac{\partial(u^* \varphi)}{\partial x^*} + \frac{\partial(v^* \varphi)}{\partial y^*} = \frac{\partial}{\partial x^*} \left( \Gamma_\varphi \frac{\partial \varphi}{\partial x^*} \right) + \frac{\partial}{\partial y^*} \left( \Gamma_\varphi \frac{\partial \varphi}{\partial y^*} \right) + S_\varphi, \quad (1)$$

where  $\varphi$  stands for the dependent variables  $u^*$ ,  $v^*$ ,  $T^*$ ; and  $\Gamma_\varphi$ ,  $S_\varphi$  are the corresponding diffusion and source terms, respectively, for the general variable  $\varphi$ , as summarized in Table 1. Other parameters are defined in the Nomenclature.

The following exponential variation in kinematic viscosity (with temperature) is assumed

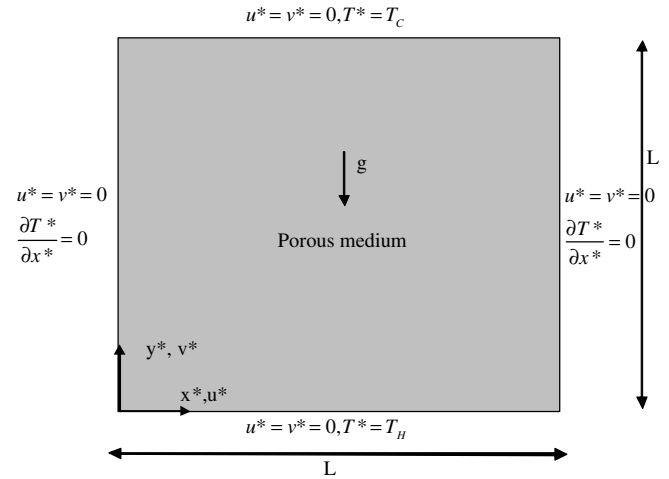


Fig. 1. Schematic of the problem under consideration.

Table 1  
Summary of the solved governing equations

Equations	$\varphi$	$\Gamma_\varphi$	$S_\varphi$
Continuity	1	0	0
$x^*$ -momentum	$u^*/\phi$	$\nu$	$-\frac{1}{\rho} \frac{\partial p^*}{\partial x^*} - \frac{\nu u^*}{K} - \frac{C_F \phi u^*  U^* }{K^{1/2}}$
$y^*$ -momentum	$v^*/\phi$	$\nu$	$-\frac{1}{\rho} \frac{\partial p^*}{\partial y^*} - \frac{\nu v^*}{K} - \frac{C_F \phi v^*  U^* }{K^{1/2}} + g\beta(T^* - T_C)$
Energy	$T^*$	$\alpha$	0

$$\eta = \frac{\nu}{\nu_C} = \exp(b\theta), \quad (2)$$

where the viscosity variation number,  $b$ , is positive/negative in case of a gas/liquid whose viscosity increases/decreases with an increase in temperature. The cold wall condition is assumed as our reference state so that  $\nu_C$  is the kinematic viscosity measured at  $T_C$ . Our dimensionless temperature is  $\theta = (T^* - T_C)/(T_H - T_C)$ . One also notes that the Taylor series expansion for very small values of  $b$  leads to linear or inverse linear relations for viscosity with temperature as

$$\begin{aligned} \nu &= \nu_C(1 + b\theta), \\ \frac{1}{\nu} &= \frac{1}{\nu_C}(1 - b\theta), \end{aligned} \quad (3-a,b)$$

similar to the models applied in [36–39].

The dimensionless stream-function is defined as

$$\begin{aligned} u &= \frac{\partial \psi}{\partial y}, \\ v &= -\frac{\partial \psi}{\partial x}. \end{aligned} \quad (4-a,b)$$

With this definition, the continuity equation is satisfied identically. The dimensionless coordinates are  $(x, y) = (x^*, y^*)/L$  and the velocity components are  $(u, v) = (u^*, v^*)(L/\alpha)$ .

Taking the curl of  $x^*$ - and  $y^*$ -momentum equations and eliminating the pressure terms, one finds the dimensionless vorticity transport equation as

$$u \cdot \nabla \omega = Pr_C((\nabla^2 \omega - \omega/Da)e^{b\theta} - A|U|\omega + S_w), \tag{5}$$

where

$$S_w = \left( \frac{\partial \eta}{\partial x} \frac{\partial \psi}{\partial x} + \frac{\partial \eta}{\partial y} \frac{\partial \psi}{\partial y} \right) / Da + A \left( \frac{\partial |U|}{\partial x} \frac{\partial \psi}{\partial x} + \frac{\partial |U|}{\partial y} \frac{\partial \psi}{\partial y} \right) + Ra_f \frac{\partial \theta}{\partial x} - \left( \frac{\partial}{\partial y} \left( \frac{\partial \eta}{\partial x} \frac{\partial^2 \psi}{\partial x \partial y} + \frac{\partial \eta}{\partial y} \frac{\partial^2 \psi}{\partial y^2} \right) + \frac{\partial}{\partial x} \left( \frac{\partial \eta}{\partial x} \frac{\partial^2 \psi}{\partial x^2} + \frac{\partial \eta}{\partial y} \frac{\partial^2 \psi}{\partial x \partial y} \right) - \frac{\partial \eta}{\partial x} \frac{\partial \omega}{\partial x} - \frac{\partial \eta}{\partial y} \frac{\partial \omega}{\partial y} \right). \tag{6}$$

The Rayleigh–Darcy number, or simply *Ra* hereafter, is defined as  $Ra = DaRa_f$ .

The vorticity directed in *z* direction is defined as

$$\omega = -\nabla^2 \psi. \tag{7}$$

The thermal energy equation now takes the following form:

$$u \cdot \nabla \theta = \nabla^2 \theta. \tag{8}$$

The average Nusselt number, as the ratio of the actual heat transfer to that of pure conduction, is defined as [3]

$$Nu = \int_0^1 \frac{\partial \theta(x, 0)}{\partial y} dx. \tag{9-a}$$

The problem is now to solve Eqs. (5–9) subject to no-slip boundary condition on the walls, i.e.  $u = v = 0$ , and the following thermal boundary conditions

$$\begin{aligned} \frac{\partial \theta}{\partial x} &= 0; && \text{vertical walls,} \\ \theta &= 0; && \text{top wall,} \\ \theta &= 1; && \text{bottom wall.} \end{aligned} \tag{9-b-d}$$

### 3. Numerical details

Numerical solutions to the governing equations for vorticity, stream-function, and dimensionless temperature are obtained by finite difference method, using the Gauss–Seidel technique with SOR. The governing equations are discretized by applying second-order accurate central difference schemes. For the numerical integration, algorithms based on the trapezoidal rule are employed similar to [40]. Details of the vorticity-stream-function method, and applied boundary conditions may be found in [41] and are not repeated here.

All runs were performed on a 61 × 61 grid. The Darcy number ranges from 10<sup>-6</sup> to 10<sup>-3</sup> while the reference Prandtl number is fixed at unity similar to Merrikh and

Mohamad [9]. The inertia coefficient,  $C_F$  is fixed at 0.56 similar to Lage [4]. Grid independence was verified by running different combinations of *Da*, *Ra<sub>f</sub>*, and *b* on three different grid sets 41 × 41, 61 × 61 and 91 × 91. Less than 1% difference between results obtained on different grids is observed. The convergence criterion (maximum relative error in the values of the dependent variables between two successive iterations) in all runs was set at 10<sup>-5</sup>.

A test on the accuracy of the numerical procedure is provided by comparing the results against those for special cases quoted in the literature, i.e. [42–45]. This comparison for the average Nusselt number and the maximum stream-function value is shown in Tables 2 and 3, respectively.

### 4. Results and discussion

Figs. 2 and 3 are designed to reflect the effects of the key parameters (being *b*, *Da*, *Ra*, and *Ra<sub>f</sub>* on isotherms and streamlines. The porous medium Rayleigh number, *Ra*, is 50 and 300, respectively, for Figs. 2 and 3. Both extreme positive and negative values of *b* are included to represent fluids with viscosities increasing and decreasing with temperature. The results of isotherms and streamlines for different values of *Da* (*Da* = 10<sup>-3</sup> and 10<sup>-4</sup>) are plotted on different charts in each figure. To maintain a constant *Ra* value, the value of *Ra<sub>f</sub>* is altered along with *Da*. One can easily see that with negative values of *b*, representing viscosity decreasing with an increase in temperature, the flow patterns are stronger. On the other hand, the converse can be deduced with positive values of *b*. The constant property solution is mostly found to be somewhere between the two cases, as expected. In all of our contour plots the contours are plotted at equal increments of the plotted variable. Comparing Figs. 2 and 3, it is clear that with a fixed value of *Da*, an increase in either *Ra* or *Ra<sub>f</sub>* leads to stronger convective flows, as expected. Examining the streamlines, which are normalized by  $\psi_{max}$ , it is quite clear that with

Table 3  
Present  $\psi_{max}$  values for  $Da = 10^{-6}$  versus those in the literature for the Darcy model

<i>Ra</i>	Present	Ref. [45]	Ref. [43]
50	2.096	2.092	2.112
100	5.319	5.359	5.377
200	8.845	8.931	8.942
250	10.131	10.244	10.253
300	11.252	11.394	11.405

Table 2  
Present *Nu* values for  $Da = 10^{-6}$  versus those in the literature for the Darcy model

<i>Ra</i>	Present	Ref. [45]	Ref. [42]	Ref. [43]	Ref. [4] ( $Da = 10^{-6}$ )
50	1.464	1.443	1.45	–	1.44
100	2.643	2.631	2.676	2.651	2.62
200	3.782	3.784	3.813	3.808	3.762
250	4.15	4.167	–	–	4.139
300	4.456	4.487	–	4.514	–

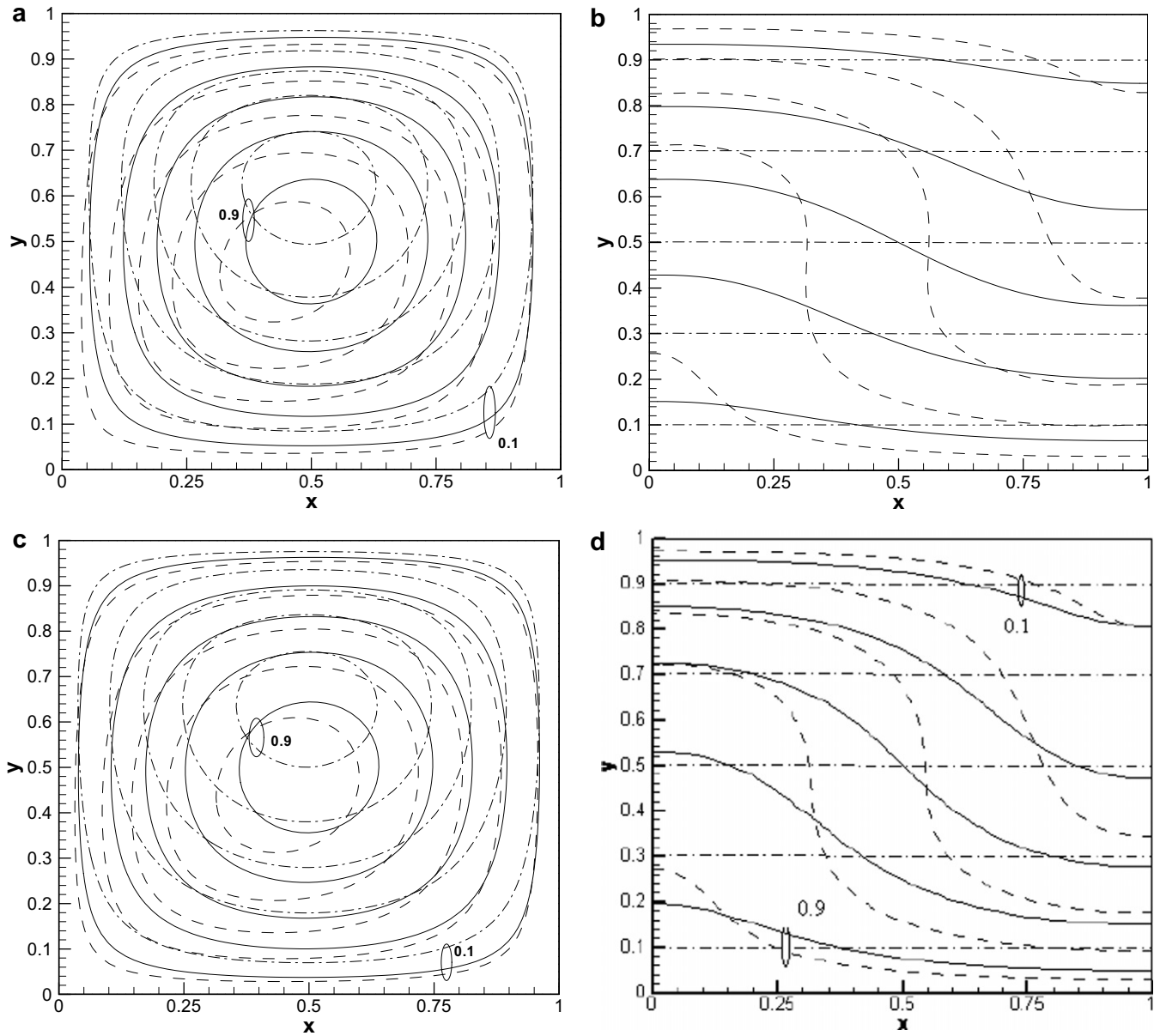


Fig. 2. (a) Streamlines for  $Ra = 50$  and  $Da = 0.001$ ,  $Ra_f = 50,000$  (for Figs. 2–3 dashed, solid, and dash-dotted lines represent  $b = -2, 0,$  and  $2$ , respectively). (b) Isotherms for  $Ra = 50$  and  $Da = 0.001$ ,  $Ra_f = 50,000$ . (c) Streamlines for  $Ra = 50$  and  $Da = 0.0001$ ,  $Ra_f = 500,000$ . (d) Isotherms for  $Ra = 50$  and  $Da = 0.0001$ ,  $Ra_f = 500,000$ .

positive values of  $b$  the core region moves toward the cold wall while with positive counterparts this region tends to be stretched downward to form an elliptical pattern and this elliptical pattern is more identifiable for  $Ra = 300$ . Moreover, with this Rayleigh number, moving from constant property to  $b = -2$ , the change in the size of the core region is less than the one associated with the change in the opposite direction, i.e. from  $b = 0$  to  $b = 2$ . For  $Ra = 50$  and  $b = 2$ , with either values of  $Da = 10^{-3}$  or  $10^{-4}$ , the isotherms are nearly horizontal implying that there is no convection flow. On the other hand, with  $b = -2$  compared to the other two values of  $b$ , regardless of  $Ra$  and  $Da$  values, the convection patterns are stronger

and isotherms are more stretched towards the horizontal walls.

Fig. 4 shows the line diagrams of the dimensionless horizontal mid-plane velocity,  $v(x, 0.5)$ , when  $b$  varies from  $-2$  to  $2$  with  $Da = 10^{-3}$  and for two cases of  $Ra = 50$  and  $300$ . As expected, a higher value of  $Ra$  promotes mixing and this is manifested as an increase in the maximum vertical velocity. It is interesting to note that with  $b = 2$  the flow nearly subsides, with the mid-plane velocity vanishing across the entire section, while for  $b = -2$  the peak is nearly five times higher than that of the constant property case. However, for  $Ra = 300$ , the ratio of the velocity peaks is not that high and it figures out at 1.5, approximately.

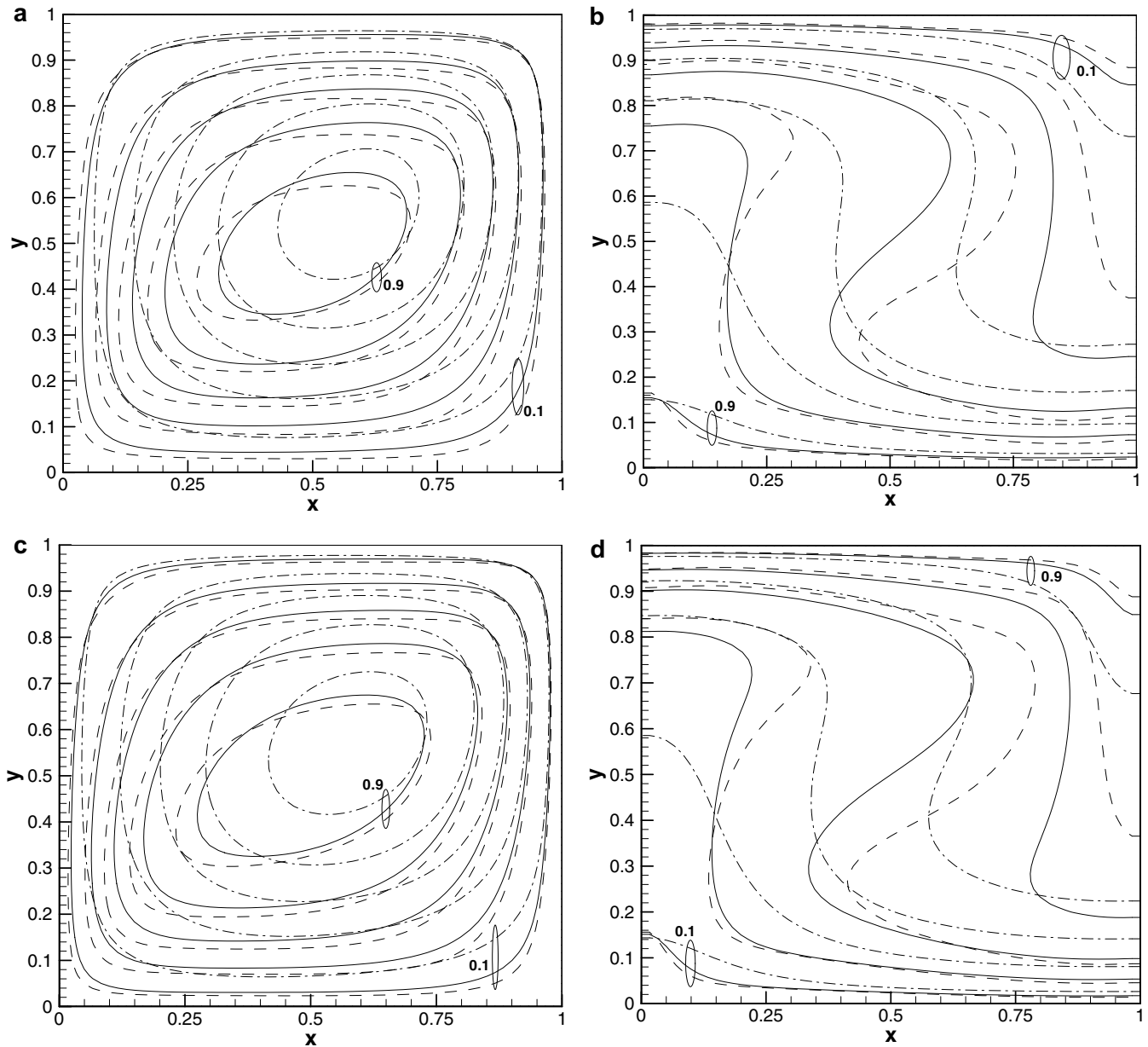


Fig. 3. (a) Streamlines for  $Ra = 300$  and  $Da = 0.001$ ,  $Ra_f = 300,000$ . (b) Isotherms for  $Ra = 300$  and  $Da = 0.001$ ,  $Ra_f = 300,000$ . (c) Streamlines for  $Ra = 300$  and  $Da = 0.0001$ ,  $Ra_f = 3,000,000$ . (d) Isotherms for  $Ra = 300$  and  $Da = 0.0001$ ,  $Ra_f = 3,000,000$ .

Fig. 5 shows the dependence of  $Nu$  and  $\psi_{\max}$  on  $b$  for different values of  $Da$  and  $Ra$ .  $Nu = 1$  means the actual heat transfer is due to conduction only, i.e.  $Nu$  only exceeds 1 when there is convection. As seen, both  $Nu$  and  $\psi_{\max}$  decrease with an increase in the absolute value of  $b$ . It is interesting that with  $Ra = 50$ , for which a convective flow pattern is expected based on constant property solutions, with positive  $b$  values of 0.1, 0.4, and 0.5 the flow nearly subsides, for  $Da$  values of  $10^{-3}$ ,  $10^{-4}$ , and  $10^{-6}$ , respectively. This observation is based on the near-unity Nusselt numbers (Fig. 5a) suggesting the dominance of the conduction heat transfer and the stream-function values (Fig. 5b) calculated much lower than their constant property counterparts. However, for  $Ra = 100$  the value of  $b$  needs to

be as high as 1.7 for the same phenomenon to occur. It is observed that increasing  $Ra$ , raises the  $Nu$  level but, interestingly, moving to other  $Ra$  values with a fixed  $Da$ , the slope of  $Nu$ - $b$  plots will remain almost the same. Interestingly,  $\psi_{\max}$  shows similar behavior; however, it is observed that for the lowest Darcy value,  $Da = 10^{-6}$ , the  $\psi_{\max}$ - $b$  curve becomes a concave one instead of the convex distribution formed for higher  $Da$  values.

Based on the observation that the  $Nu$ - $b$  plots are parallel for a fixed  $Da$  with changing  $Ra$ , it is tempting to argue that defining an average Rayleigh number, the  $Nu$ - $Ra$  relation could remain, to a good approximation, independent of the changes in viscosity. In the preceding discussion, the Rayleigh numbers were calculated at the cold wall

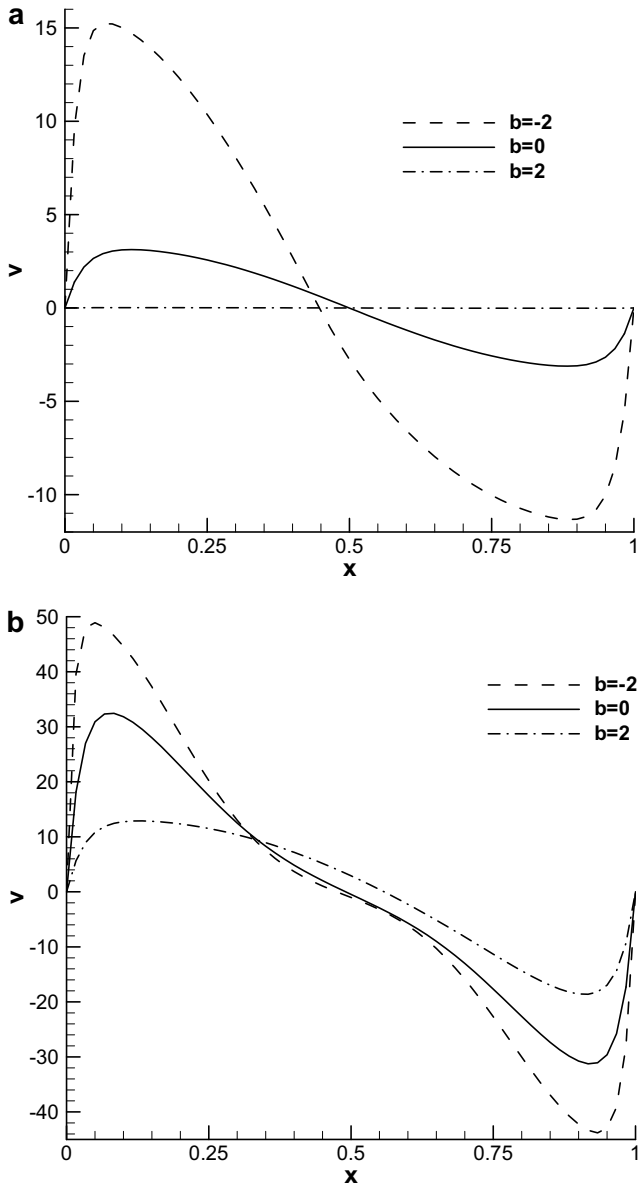


Fig. 4. (a) The dimensionless horizontal mid-plane velocity versus  $x$  for  $Ra = 50$  and  $Da = 10^{-3}$ . (b) The dimensionless horizontal mid-plane velocity versus  $x$  for  $Ra = 300$  and  $Da = 10^{-3}$ .

temperature. The apparent destabilizing effect of decreasing viscosity was observed in all figures when the Rayleigh number was calculated this way. Let us now see what happens when an average/effective Rayleigh number is used. It is instructive to note that there are two approaches to account for variable property (forced or natural convection) problems. The first one is evaluating the fluid property at a reference temperature. The second one is evaluating the fluid property at a reference temperature and using a correction factor to account for property variations. More details may be found in Kakaç and Yener [29].

Nield [30] recommends using a harmonic average for the fluid viscosity in the effective Rayleigh number. Since the

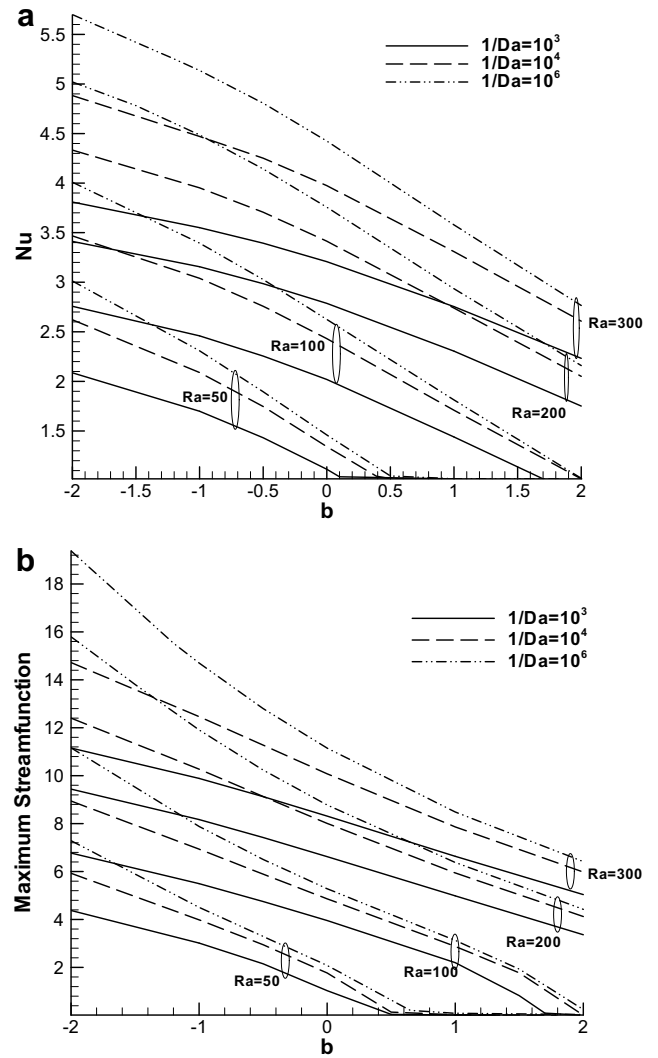


Fig. 5. (a) and (b) Plots of  $Nu$  and  $\psi_{max}$  versus  $b$  for different values of  $Da$  and  $Ra$ .

Rayleigh number is inversely proportional to viscosity, we define our effective Rayleigh number as the arithmetic mean of the Rayleigh numbers at two extreme temperatures

$$Ra_{eff} = \left( \frac{Ra_C + Ra_H}{2} \right). \quad (10)$$

The subscripts ‘H’ and ‘C’ are applied to show that heated and cooled wall temperatures are applied to evaluate the viscosity. One notes that  $Ra_C = Ra$ , as applied so far, and that using Eq. (2) one has

$$Ra_{eff} = Ra(1 + \exp(-b))/2. \quad (11)$$

The effective Rayleigh numbers calculated by the above equation are shown in our Table 4 as Case 1.

On the other hand, Guo and Zhao [28] proposed the arithmetic mean temperature as the reference temperature and evaluated the viscosity at that temperature. However, when using this mean temperature, the Nusselt number

Table 4-A

Calculation of the effective and average Rayleigh numbers and  $Nu/Nu_{cp}$  for ( $Da = 10^{-3}$ ,  $Ra = 50$ )

$b$	Numerical	Case 1			Case 2		
	$Nu/Nu_{cp}$	$Ra_{eff}$	$Nu/Nu_{cp}$	$E$ (%)	$Ra_{am}$	$Nu/Nu_{cp}$	$E$ (%)
-2	1.845	209.73	2.517	36.42	135.92	2.07	12.17
-0.5	1.266	66.22	1.327	4.82	64.2	1.291	1.97
0.5	0.899	40.16	0.9	0.11	38.94	0.893	0.67

showed notable differences from the constant property case. This behavior could be expected, to some extent, in the light of [32], where the authors recommended, for the clear fluid case, adding a viscosity fraction to the constant property  $Nu$ – $Ra$  correlations to make them useful in variable property cases.

All in all, for this case, the average Rayleigh number reads

$$Ra_{am} = Ra \exp(-0.5b), \quad (12)$$

wherein  $Ra_{am}$  is the Rayleigh number with the viscosity being evaluated at the arithmetic mean temperature and is referred to as Case 2 in Table 4.

Using the Taylor series, it is an easy task to show that for small  $b$  values both of the two approaches lead to the same answer being

$$Ra_{am} = Ra_{eff} = Ra(1 - 0.5b). \quad (13)$$

Nonetheless, for higher values of  $b$  the two methods will lead to very different results as shown in Table 4 which lists the ratio of the variable property Nusselt number divided by that of constant property,  $Nu/Nu_{cp}$ , versus average/effective Rayleigh number. As seen, the results are closer for small values of  $b$ , however, increasing  $b$  not only the two methods will diverge but also they lead to erroneous results compared to our numerical solutions. It could be concluded that the concept of an effective Rayleigh number, though proven to be useful to show the onset of convection for a porous layer heated from below, is restricted to the case where an inverse linear viscosity–temperature relation is assumed (and is equivalent to our model with very small  $b$  according to Eq. (3)). On the other hand, the average Rayleigh number approach leads to better results for low  $Ra$  and  $b$  cases and increasing either of the two parameters restricts the application of this method. According to Table 4, none of the above methods are accurate and there is a need for another alternative.

The issue is finding a reference temperature to evaluate the viscosity so that the results will be valid for the entire

$b$ -domain that is considered in this analysis. Based on our numerical results, it is reasonable to expect this reference temperature to change with the porous medium permeability, which may be represented by the Darcy number. By observation of the results, we have found this reference temperature to change with the Darcy number as follows

$$\begin{aligned} T_{ref} &= T_C + 0.45(T_H - T_C) \quad \text{for } Da = 10^{-6}, \\ T_{ref} &= T_C + 0.4(T_H - T_C) \quad \text{for } Da = 10^{-4}, \\ T_{ref} &= T_C + 0.35(T_H - T_C) \quad \text{for } Da = 10^{-3}. \end{aligned} \quad (14\text{-a,b,c})$$

Substitution of the above reference temperature in Eq. (2), will lead to the following average Rayleigh numbers

$$\begin{aligned} Ra_{ave} &= Ra_C \exp(-0.45b) \quad \text{for } Da = 10^{-6}, \\ Ra_{ave} &= Ra_C \exp(-0.4b) \quad \text{for } Da = 10^{-4}, \\ Ra_{ave} &= Ra_C \exp(-0.35b) \quad \text{for } Da = 10^{-3}. \end{aligned} \quad (15\text{-a,b,c})$$

Table 5 is designed to show the results of our constant property calculation with viscosity being evaluated at the above reference temperature. It seems that our predictions are within good agreement with the maximum error of 10% for  $Nu$  and 12% for  $\psi_{max}$  for the extreme viscosity variation cases. It may be concluded that one can still apply the constant property solutions available in the literature with the only modification that the fluid property needs to be evaluated at the reference temperature recommended here. Another point worthy of comment is that our results are limited within a range of the Darcy numbers being those relevant to clear fluid ( $1/Da \rightarrow 0$ ) and Darcy flow model ( $Da \rightarrow 0$ ). For these two cases the reference temperatures are  $T_{ref} = T_C + 0.5(T_H - T_C)$  and  $T_{ref} = T_C + 0.25(T_H - T_C)$  with the former being recommended indirectly by Nield [30] (for small values of  $b$ ) for the Darcy flow model and the latter proposed by Zhong et al. [33] for the clear fluid natural convection in a laterally heated box. It is interesting that though the flow structure is completely different in a lateral and bottom heating case, as noted by Nield [46] and implied by Bejan [41], the limiting

Table 4-B

Calculation of the effective and average Rayleigh numbers and  $Nu/Nu_{cp}$  for ( $Da = 10^{-4}$ ,  $Ra = 100$ )

$b$	Numerical	Case 1			Case 2		
	$Nu/Nu_{cp}$	$Ra_{eff}$	$Nu/Nu_{cp}$	$E$ (%)	$Ra_{am}$	$Nu/Nu_{cp}$	$E$ (%)
-2	1.4264	419.45	1.8219	27.73	271.83	1.579	10.72
-1	1.25	185.91	1.362	8.9	164.87	1.2922	3.35
1	0.703	68.39	0.766	8.9	60.65	0.688	2.1



Table 5  
Application of the reference temperature approach adopted here for some values of  $Da$ ,  $Ra$ , and  $b$

$Da$	$Ra$	$b$	$Ra_{ave}$	$Nu^*$	$Nu$	$e_{Nu}$ (%)	$\psi_{max}^*$	$\psi_{max}$	$e_{\psi_{max}}$ (%)
$10^{-6}$	50	-2	122.98	2.963	3.013	1.66	6.486	7.206	9.99
		-1	78.42	2.223	2.308	3.68	4.162	4.505	7.61
	100	-2	245.96	4.096	4.01	2.14	9.991	11.162	10.49
		-1	156.83	3.359	3.395	1.06	7.483	7.882	5.33
		1	63.76	1.863	1.813	2.71	3.2	3.128	5.06
	200	-2	491.92	5.248	5.02	4.54	14.51	15.797	8.15
		-1	313.66	4.498	4.486	0.27	11.429	11.911	4.05
		1	127.53	3.02	2.93	2.93	6.445	6.38	1.01
	300	2	81.31	2.283	2.16	5.71	4.329	4.423	2.12
		-1	470.49	5.177	5.14	0.71	14.173	14.702	3.59
		1	191.29	3.684	3.58	2.91	8.533	8.486	0.55
		2	121.97	2.95	2.77	6.5	6.227	6.416	2.94
$10^{-4}$	50	-2	111.28	2.584	2.62	1.37	5.32	5.928	10.23
		-1	74.59	1.994	2.08	4.12	3.624	3.984	9.04
	100	-2	222.55	3.563	3.47	2.86	8.536	8.941	4.53
		-1	149.18	3.004	3.04	1.2	6.629	6.933	4.38
		1	67.03	1.828	1.71	6.89	3.156	2.878	9.66
	200	-2	445.11	4.507	4.34	3.85	12.287	12.4	0.91
		-1	298.36	3.974	3.953	0.54	10.07	10.272	1.97
		1	134.06	2.84	2.74	3.64	6.169	5.941	3.83
	300	2	89.87	2.274	2.1	8.29	4.404	4.124	6.79
		-1	447.55	4.514	4.471	0.96	12.318	12.465	1.18
		1	201.1	3.414	3.31	3.14	8.009	7.863	1.85
		2	134.8	2.84	2.61	8.8	6.169	5.981	3.15
$10^{-3}$	50	-2	100.69	2.027	2.086	2.83	3.981	4.374	8.98
		-1	70.95	1.592	1.69	5.8	2.74	3.011	9
	100	-2	201.38	2.79	2.758	1.16	6.622	6.769	2.17
		-1	141.91	2.417	2.459	1.71	5.276	5.495	3.99
		1	70.47	1.587	1.442	10	2.612	2.375	9.97
	200	2	49.66	1.11	1.03	7.77	0.911	0.824	10
		-2	402.76	3.505	3.412	2.72	9.619	9.44	1.9
		-1	283.81	3.151	3.156	0.2	8.074	8.168	1.15
		1	140.94	2.41	2.305	4.56	5.27	4.986	5.69
	300	2	99.32	2.01	1.827	10	3.901	3.535	10.35
		-1	425.72	3.559	3.551	0.25	9.873	9.885	0.12
		1	211.41	2.846	2.755	3.3	6.486	6.633	2.22
2		148.98	2.469	2.244	10	5.463	5.037	8.46	

reference temperature for the clear fluid case is the same. The dependence of the reference temperature on the Darcy number is expected as each  $Da$  value is associated with a unique convection pattern. For the sake of simplicity, we propose a rough and ready estimation for the dependence of the reference temperature on the Darcy number as follows

$$T_{ref} = T_C + 0.5(1 - 0.848Da^{0.15})(T_H - T_C). \tag{16}$$

This is found by fitting a power-curve ( $\sim Da^q$ ) on the coefficients used in Eq. (14a-c).

The average Rayleigh number, Eq. (15), now takes the following form

$$Ra_{ave} = Ra_C \exp(-0.5b(1 - 0.848Da^{0.15})). \tag{17}$$

However, one should be warned that these last two equations are valid for the range of the Darcy number considered in our study being  $10^{-3}$ – $10^{-6}$ . One notes that for small values of  $b$  with  $Da = 0$  the average Rayleigh number tends to the effective Rayleigh number of Nield [30].

### 5. Conclusion

Numerical simulation of Bénard natural convection in a bottom heated porous-saturated square enclosure is presented based on the general momentum equation. The exponential model for the variation of viscosity with the temperature is applied. A reference temperature approach is undertaken to account for viscosity variation. It is found that the reference temperature, at which the fluid properties should be evaluated, is a decreasing function of the Darcy number and is approximately independent of the other parameters considered here. Applying this reference temperature, one can still use the constant property results and this, in turn, will reduce the computational time and expense required for solving a variable property problem.

### Acknowledgments

The first author, the scholarship holder, acknowledges the support provided by The University of Queensland

in terms of UQILAS, Endeavor IPRS, and School Scholarship.

## References

- [1] G. Lauriat, V. Prasad, Non-Darcian effects on natural-convection in a vertical porous enclosure, *Int. J. Heat Mass Transfer* 32 (1989) 2135–2148.
- [2] N. Kladias, V. Prasad, Flow transitions in buoyancy-induced non-Darcy convection in a porous-medium heated from below, *J. Heat Transfer – Trans. ASME* 112 (1990) 675–684.
- [3] S.A. Khashan, A.M. Al-Amiri, I. Pop, Numerical simulation of natural convection heat transfer in a porous cavity heated from below using a non-Darcian and thermal non-equilibrium model, *Int. J. Heat Mass Transfer* 49 (2006) 1039–1049.
- [4] J.L. Lage, Effect of the convective inertia term on Benard convection in a porous-medium, *Numer. Heat Transfer A* 22 (1992) 469–485.
- [5] K. Vafai, C.L. Tien, Boundary and inertia effects on flow and heat-transfer in porous-media, *Int. J. Heat Mass Transfer* 24 (1981) 195–203.
- [6] C.T. Hsu, P. Cheng, Thermal dispersion in a porous-medium, *Int. J. Heat Mass Transfer* 33 (1990) 1587–1597.
- [7] A.A. Merrikh, J.L. Lage, A.A. Mohamad, Natural convection in nonhomogeneous heat-generating media: Comparison of continuum and porous-continuum models, *J. Porous Media* 8 (2005) 149–163.
- [8] A.A. Merrikh, A.A. Mohamad, Transient natural convection in differentially heated porous enclosures, *J. Porous Media* 3 (2000) 165–178.
- [9] A.A. Merrikh, A.A. Mohamad, Non-Darcy effects in buoyancy driven flows in an enclosure filled with vertically layered porous media, *Int. J. Heat Mass Transfer* 45 (2002) 4305–4313.
- [10] C. Beckermann, R. Viskanta, S.A. Ramadhani, A numerical study of non-Darcian natural-convection in a vertical enclosure filled with a porous-medium, *Numer. Heat Transfer* 10 (1986) 557–570.
- [11] J.R. Figueiredo, J. Llagostera, Comparative study of the unified finite approach exponential-type scheme (UNIFAES) and its application to natural convection in a porous cavity, *Numer. Heat Transfer B* 35 (1999) 347–367.
- [12] Z.L. Guo, T.S. Zhao, A lattice Boltzmann model for convection heat transfer in porous media, *Numer. Heat Transfer B* 47 (2005) 157–177.
- [13] S.C. Hirata, B. Goyeau, D. Gobin, R.M. Cotta, Stability of natural convection in superposed fluid and porous layers using integral transforms, *Numer. Heat Transfer B* 50 (2006) 409–424.
- [14] G.B. Kim, J.M. Hyun, Buoyant convection of a power-law fluid in an enclosure filled with heat-generating porous media, *Numer. Heat Transfer A* 45 (2004) 569–582.
- [15] B.V.R. Kumar, M. Shalini, Natural convection in a thermally stratified wavy vertical porous enclosure, *Numer. Heat Transfer A* 43 (2003) 753–776.
- [16] A. Mansour, A. Amahmid, M. Hasnaoui, M. Bourich, Multiplicity of solutions induced by thermosolutal convection in a square porous cavity heated from below and submitted to horizontal concentration gradient in the presence of solet effect, *Numer. Heat Transfer A* 49 (2006) 69–94.
- [17] M.C.C. Mojtabi, Y.P. Razi, K. Maliwan, A. Mojtabi, Influence of vibration on solet-driven convection in porous media, *Numer. Heat Transfer A* 46 (2004) 981–993.
- [18] V. Prasad, A. Tuntomo, Inertia effects on natural-convection in a vertical porous cavity, *Numer. Heat Transfer* 11 (1987) 295–320.
- [19] K. Slimi, A. Mhimid, M. Ben Salah, S. Ben Nasrallah, A.A. Mohamad, L. Storesletten, Anisotropy effects on heat and fluid flow by unsteady natural convection and radiation in saturated porous media, *Numer. Heat Transfer A* 48 (2005) 763–790.
- [20] K. Slimi, L. Zili-Ghedira, S. Ben Nasrallah, A.A. Mohamad, A transient study of coupled natural convection and radiation in a porous vertical channel using the finite-volume method, *Numer. Heat Transfer A* 45 (2004) 451–478.
- [21] P. Vasseur, C.H. Wang, M. Sen, The Brinkman model for natural-convection in a shallow porous cavity with uniform heat-flux, *Numer. Heat Transfer* 15 (1989) 221–242.
- [22] H. Beji, D. Gobin, Influence of thermal dispersion on natural-convection heat-transfer in porous-media, *Numer. Heat Transfer A* 22 (1992) 487–500.
- [23] A.M. Al-Amiri, Natural convection in porous enclosures: The application of the two-energy equation model, *Numer. Heat Transfer A* 41 (2002) 817–834.
- [24] G. Lin, C.B. Zhao, B.E. Hobbs, A. Ord, H.B. Muhlhaus, Theoretical and numerical analyses of convective instability in porous media with temperature-dependent viscosity, *Commun. Numer. Meth. Eng.* 19 (2003) 787–799.
- [25] J.Y. Jang, J.S. Leu, Buoyancy-induced boundary-layer flow of liquids in a porous-medium with temperature-dependent viscosity, *Int. Commun. Heat Mass Transfer* 19 (1992) 435–444.
- [26] J.Y. Jang, J.S. Leu, Variable viscosity effects on the vortex instability of free-convection boundary-layer flow over a horizontal surface in a porous-medium, *Int. J. Heat Mass Transfer* 36 (1993) 1287–1294.
- [27] D.R. Kassoy, A. Zebib, Variable viscosity effects on onset of convection in porous-media, *Phys. Fluids* 18 (1975) 1649–1651.
- [28] Z.L. Guo, T.S. Zhao, Lattice Boltzmann simulation of natural convection with temperature-dependent viscosity in a porous cavity, *Prog. Comput. Fluid Dyn.* 5 (2005) 110–117.
- [29] S. Kakaç, Y. Yener, *Convective Heat Transfer*, CRC Press, Boca Raton, 1995.
- [30] D.A. Nield, Estimation of an effective Rayleigh number for convection in a vertically inhomogeneous porous-medium or clear fluid, *Int. J. Heat Fluid Flow* 15 (1994) 337–340.
- [31] D.A. Nield, The effect of temperature-dependent viscosity on the onset of convection in a saturated porous medium, *J. Heat Transfer – Trans. ASME* 118 (1996) 803–805.
- [32] T.Y. Chu, C.E. Hickox, Thermal-convection with large viscosity variation in an enclosure with localized heating, *J. Heat Transfer – Trans. ASME* 112 (1990) 388–395.
- [33] Z.Y. Zhong, K.T. Yang, J.R. Lloyd, Variable property effects in laminar natural-convection in a square enclosure, *J. Heat Transfer – Trans. ASME* 107 (1985) 133–138.
- [34] D.L. Siebers, R.F. Moffatt, R.G. Schwind, Experimental, variable properties natural-convection from a large, vertical, flat surface, *J. Heat Transfer – Trans. ASME* 107 (1985) 124–132.
- [35] T.M. Harms, M.A. Jog, R.M. Manglik, Effects of temperature-dependent viscosity variations and boundary conditions on fully developed laminar forced convection in a semicircular duct, *J. Heat Transfer – Trans. ASME* 120 (1998) 600–605.
- [36] D.A. Nield, A.V. Kuznetsov, Effects of temperature-dependent viscosity in forced convection in a porous medium: Layered-medium analysis, *J. Porous Media* 6 (2003) 213–222.
- [37] D.A. Nield, D.C. Porneala, J.L. Lage, A theoretical study, with experimental verification, of the temperature-dependent viscosity effect on the forced convection through a porous medium channel, *J. Heat Transfer – Trans. ASME* 121 (1999) 500–503.
- [38] K. Hooman, Entropy-energy analysis of forced convection in a porous-saturated circular tube considering temperature-dependent viscosity effects, *Int. J. Exergy* 3 (2006) 436–451.
- [39] K. Hooman, H. Gurgenci, Effects of temperature-dependent viscosity variation on entropy generation, heat, and fluid flow through a porous-saturated duct of rectangular cross-section, *Appl. Math. Mech. (Eng. ed.)* 28 (2007) 69–76.
- [40] K. Hooman, A perturbation solution for forced convection in a porous saturated duct, *J. Comput. Appl. Math.*, in press (Doi: doi:10.1016/j.cam.2006.11.005).
- [41] A. Bejan, *Convection Heat Transfer*, Wiley, Hoboken, NJ, 1984.
- [42] V. Prasad, F.A. Kulacki, Natural-convection in horizontal porous layers with localized heating from below, *J. Heat Transfer – Trans. ASME* 109 (1987) 795–798.

- [43] J.P. Caltagirone, Thermoconvective instabilities in a horizontal porous layer, *J. Fluid Mech.* 72 (1975) 269–287.
- [44] G. Schubert, J.M. Straus, 3-Dimensional and multicellular steady and unsteady convection in fluid-saturated porous-media at high Rayleigh numbers, *J. Fluid Mech.* 94 (1979) 25–38.
- [45] E. Bilgen, M. Mbaye, Benard cells in fluid-saturated porous enclosures with lateral cooling, *Int. J. Heat Fluid Flow* 22 (2001) 561–570.
- [46] D.A. Nield, The modeling of viscous dissipation in a saturated porous medium, *J. Heat Transfer – Trans. ASME*, in press.